Tomographic evaluation of the bronchial and pulmonary vascular relationships in cats naturally infected of heartworm

Student:
Carla Beatriz Gutiérrez Ramos

Tutor:
José Alberto Montoya Alonso

Collaborating tutor:
Sara Nieves García Rodríguez

Co-tutor:
Mario Óscar Encinoso Quintana

Academic year: 2022-2023
(Ordinary Call)

UNIVERSIDAD DE LAS PALMAS DE GRAN CANARIA
Facultad de Veterinaria

INDEX

ABSTRACT

Feline dirofilariosis mainly differs to canine dirofilariosis because of the great response of the animal against the worm infection (*Dirofilaria immitis*), producing an intense lung inflammatory reaction, developing what is known as "Heartworm Associated Respiratory Disease" (HARD). This inflammation can alter the vasculature and bronchial structure of the lung. Computed tomography (CT) is increasingly present in veterinary medicine, being helpful in the diagnosis of feline thorax pathologies. The measurement of the bronchial lumen to pulmonary artery (BA), bronchial lumen to pulmonary vein (BV) and pulmonary vein to pulmonary artery (PV/PA) ratios are of great relevance to recognise changes in the different pulmonary structures. The aim of this study was to analyse these ratios in cats naturally infected with *D. immitis* in order to evaluate the damages this disease generates in this species. Considering the age, breed and sex data, 24 animals were analysed to assess the BA, BV and PV/PA measurements with CT scan, differentiating between animals diagnosed with HARD (18) and healthy animals (6). Significant changes were not observed in the diameter of the arteries of infected cats, thus not showing signs of pulmonary hypertension. Contrarily, bronchi were affected, so the BA ratio could be used to determine those altered in cats with bronchiectasis due to respiratory pathologies. The BV ratio has not been previously described in cats, so these results could serve as reference values for future investigations. Furthermore, it was observed that 4 lung lobes were affected, so this ratio could also be useful to detect bronchial lumen alterations. The PV/PA ratio did not show significant differences for any of the lung lobes between the studied groups, since neither the artery nor the vein were affected by the disease. Therewith, BA and BV ratios could be of usefulness when the bronchial structure is altered by HARD, and might be practical in the diagnosis of the disease in endemic areas. Even so, more studies should be carried out to support these results.

INTRODUCTION

Dirofilariosis is a severe cardiopulmonary disease caused by the nematode *Dirofilaria immitis* (Montoya-Alonso & Carretón-Gómez, 2012). This disease mainly affects canines, being these the natural hosts. Meanwhile, cats are considered atypical hosts, since they can also become infected (Ettinger *et al*., 2017). Likewise, it is possible the transmission of the parasite to humans, thereby constituting a zoonosis (Simón *et al*., 2012). Its transmission happens through Culicidae mosquitoes of the *Aedes*, *Culex* or *Anopheles* genera, but *Culex pipiens* and *Culex theileri* are the species present in Spain. Additionally, this parasite characteristically hosts

an endosymbiotic bacterium, *Wolbachia pipientis*, which constitutes a key role in the pathogenicity of the disease (Montoya-Alonso & Carretón-Gómez, 2012).

The disease has a global distribution, being more common in tropical and semitropical regions, where high temperatures and humidity are present, since this favours the development of the mosquito population. Spain is one of the countries with the best conditions for the development of the parasite, with a mean prevalence of 6.47% in the canine species and a seroprevalence of 9.4% in the feline species. Moreover, the Balearic Islands (prevalence of 10.87% in the canine species, and 16% of seroprevalence in the feline species) and the Canary Islands (prevalence of 11.58% in the canine species, and a seroprevalence of 19.2% in the feline species) are considered hyperendemic areas (Montoya-Alonso *et al*., 2022a; Montoya-Alonso *et al*., 2022b).

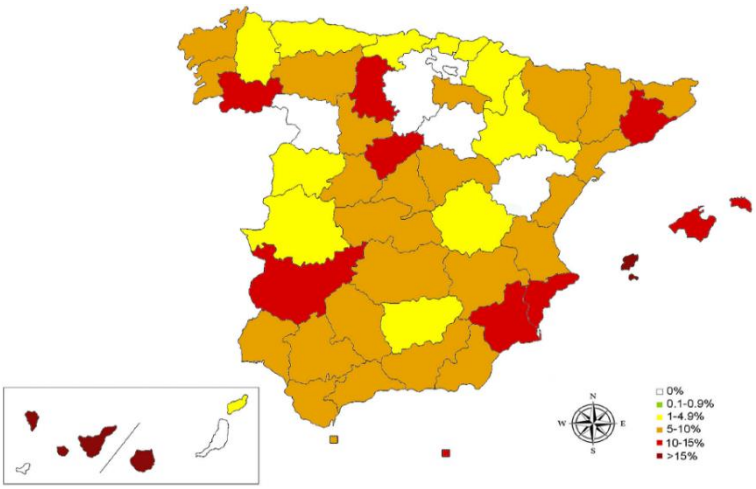

Figure 1. Seroprevalence map for* D. immitis *in cats in Spain.
Source: Montoya *et al*., 2022a

The life cycle of *D. immitis* is similar both in the cat and in the dog, but with certain differences due to the biological characteristics of the cat. The cat, as a non-natural host, has an inherent resistance to the infection, therefore being more resistant than the dog. For that reason, most of the immature larvae die when they reach the lungs, developing just a few of them (Rothrock, 2013). Thus, between 2 and 4 adult parasites most commonly develop in the cat (European Society of Dirofilariosis and Angiostrongylosis [ESDA], 2017), whereas the parasite load in the dog is variable, but much greater (Montoya-Alonso & Carretón-Gómez, 2012). Additionally, cats seldom present circulating microfilariae (10 – 20%) (Stannard, 2015), and, otherwise, they last for only a short period of time, usually no more than 228 days post-infection (Rothrock, 2013). This low incidence of microfilaraemia in cats is often due to single-sex worm infections (Stannard, 2015), impeding the reproduction of the larvae. Another influential factor in the amicrofilaraemia is the own immune-mediated response of the animal which kills them (Rothrock, 2013). (**Table 1**).

Table 1. Main differences between feline and canine dirofilariosis

	CAT	DOG
Longevity of worms	2 – 4 years	5 – 7 years
Number of worms	2 – 4 worms most common	Variable parasite burden
Resistance to infection	More resistant to infection	Less resistant to infection
Affected organs	Lungs	Lungs and heart
Ectopic infections	More frequent than in dog	Very unusual
Single-sex infections	Common	Unusual
Microfilaremia	Transient: present for about a month Seen only in 20% of cats	Persistent: present for years, even after death of adult worms Very common

Source: Montoya & Carretón, 2012; Stannard, 2015. Own elaboration

In the cat, the arrival of the immature larvae (L5) to the pulmonary arteries, approximately 3 months post-infection (Blagburn, 2019), leads to an acute inflammatory reaction in the lung, and this originates the activation of the pulmonary intravascular macrophages (PIMs), which are absent in the pulmonary vascular bed of the dogs (Ware & Ward, 2020). Following this response, most of the juvenile worms die, if not all, constituting the first presentation stage in the cat, what is known as "Heartworm Associated Respiratory Disease" (HARD) (Walden & Estrada, 2019). This gives rise to a set of clinical findings associated with the pulmonary changes that occur because of the death of the larvae, among them eosinophilic and neutrophilic pneumonia, and proliferative lesions of the pulmonary arteries and bronchioles. Furthermore, there can be oedema as a result of the increased vascular permeability of the lung and hyperplasia of alveolar type II cells, which produce surfactant, being more widespread in cats than dogs, and hampering the correct alveolar exchange of oxygen (Ware & Ward, 2020). It has been noted that when the immune system of the cat kills the immature larvae, large amounts of *Wolbachia pipientis* are released, resulting in a great antibody response against this bacterium. Thus, it is possible that *Wolbachia* spp. plays also an important role in the characteristic HARD inflammatory reactions (Morchón *et al*., 2004; Turb *et al*., 2012).

Those immature larvae that survive the immune response of the cat can develop into the adult stage. It has been proven that the adult parasites decrease the activity of the PIMs (Dillon *et al*., 2008), so the pulmonary inflammation decreases, and the symptoms usually minimise or disappear (Ware & Ward, 2020). The adult parasites can reproduce 7–8 months post-infection (Rothrock, 2013). Once the adult worms develop, the "chronic heartworm disease" (HWD)

starts, the second stage of the disease. As the adult parasites die, the PIMs are reactivated (Dillon *et al*., 2008), again causing an intense pulmonary inflammation. The disintegration of the dead worms, and fragments being swept along the small arterioles, can produce an acute damage due to pulmonary thromboembolism. For this reason, the presence of a single adult worm in the cat can have fatal consequences (Stannard, 2015).

Cats that survive may have permanent damage, as the living adults can generate villous endarteritis, fibrosis of the vascular intima and hypertrophy of the vascular wall in the pulmonary arteries (Montoya-Alonso & Carretón-Gómez, 2012), manifesting narrowed and tortuous pulmonary vessels. Besides, cats have a smaller pulmonary arterial tree, hence less pulmonary collateral circulation, and consequently favouring pulmonary infarction with infections of small number of adult worms (Rothrock, 2013). Previous studies have shown that parasitised cats are not prone to developing right ventricular hypertrophy, as it occurs in dogs; but there can be a loss of the collagen content in the myocardium of the right ventricle, related to the severity of the pulmonary disease (Winter *et al*., 2017). Additionally, caval syndrome and tricuspid valve regurgitation are uncommon manifestations (Rothrock, 2013). Lastly, unlike the dog, it has been reported more frequently in cats aberrant migrations of the parasite, reaching the eye, central nervous system, systemic arteries and subcutaneous tissue (ESDA, 2017).

The reported clinical signs in both presentation forms of the disease are considered very similar to other pathologies, as feline asthma and chronic bronchitis, being confused and misdiagnosed frequently (Rothrock, 2013). During these stages, the cat can show respiratory symptoms as coughing and/or dyspnoea, mainly. Occasionally, gastrointestinal symptoms, as vomiting unrelated to food intake, or neurological signs, may be present. Also, a lot of cats are asymptomatic or have unspecific clinical signs. Sudden death caused by pulmonary thromboembolism has been reported in up to 20% of the affected cats (ESDA, 2017; Blagburn, 2019; American Heartworm Society, 2020; Ware & Ward, 2020). (**Table 2**).

Table 2. More frequent clinical signs in feline cardiopulmonary dirofilariosis

CLINICAL SIGNS	FREQUENCY
Dyspnoea	48%
Cough	38%
Vomiting	16-33%
Sudden death	10-20%
Neurological signs	14%
Asymptomatic	28%

Source: Montoya & Carretón, 2012. Own elaboration

As for the feline cardiopulmonary dirofilariosis diagnosis, it is considered much more complicated than in the canine species, since cats are usually asymptomatic and, even showing symptoms, they are not pathognomonic of the disease, being on occasion unspecific (ESDA, 2017). In endemic areas, this disease should be included in the differential diagnoses of cats with compatible symptoms (Montoya-Alonso & Carretón-Gómez, 2012). To reach the final diagnosis, a combination of several tests is needed, among which are included serological techniques, thoracic radiographies and echocardiography (Ware & Ward, 2020).

Since cats seldom have microfilaraemia, its analysis, through thick blood smear or the Knott test, is not considered a first-choice test (American Heartworm Society, 2020).

Antigen rapid tests are highly specific, so a positive result indicates the animal has the infection (American Heartworm Society, 2020). However, false negative results are possible in cats due to single-sex infections, when such commercial test only detects adult females; presence of immature or juvenile larvae; low worm burden; as well as the formation of antigen-antibody complexes (Ware & Ward, 2020). In spite of all of this, a negative result should not be considered definitive to rule-out the disease if there is suspicion of it, so results should only be recorded as "positive" or "no antigen detected" (NAD) (ESDA, 2017; American Heartworm Society, 2020).

Antibody tests against *D. immitis* show exposure to the parasite as early as 2–3 months post-infection, since it detects antibodies against a superficial protein of L4 (Ware & Ward, 2020). However, a positive result indicates exposure to the parasite, but it does not differentiate between immature or mature forms, nor it assures there is still an infection (Stannard, 2015). Thus, with a positive test, complementary tests should be done to support such result in order to confirm the diagnosis of feline cardiopulmonary dirofilariosis or HARD (Ware & Ward,

2020). This technique could be carried out with an indirect Enzyme-Linked Immunosorbent Assay (ELISA), where the antibodies against the parasite in the animal are detected, being one of the most used serologic tests globally.

Echocardiography to detect adult worms in cats is a useful complementary test, but it can be more challenging than in dogs, since they do not usually have a high worm burden, hampering the visualisation of them (Montoya-Alonso & Carretón-Gómez, 2012). Adult parasites in cats are primarily located in the main pulmonary arteries, followed by the right ventricle and atrium, and, less frequently, vena cava (DeFrancesco *et al*., 2001; Stannard, 2015). It is important to investigate all the possible locations, since they can go unnoticed due to low worm burden (American Heartworm Society, 2020). According to DeFrancesco *et al*., 2001, the use of echocardiography for the diagnosis of feline heartworm disease in cats can obtain a positive result in 40% of the animals involved.

Thorax radiography is a very effective tool to evince compatible findings with dirofilariosis, rule-out other differential diagnoses and, also, assess the severity of the disease and monitor its evolution (American Heartworm Society, 2020). Radiographic anomalies do not necessarily go in keeping with the severity of the disease and are present in over 50% of the cats with dirofilariosis (Ware & Ward, 2020). As for the radiographic findings, there can be an increase and higher tortuosity of the main and peripheric pulmonary arteries. The main segment of the pulmonary artery is not usually visible in cats, since it is also located more medial compared to dogs, hidden by the cardiac silhouette (Montoya-Alonso & Carretón-Gómez, 2012; Ware & Ward, 2020). Caudal lobal arteries are normally prominent, especially the right sided ones, since it is where worms are commonly found, better appreciated in the dorsoventral projection (Montoya-Alonso & Carretón-Gómez, 2012; Ware & Ward, 2020).

Focal, multifocal or diffuse bronchointerstitial lung patterns can be appreciated. Other findings include pulmonary infiltrates due to pulmonary thromboembolism, as well as hyperinflation of the lungs. Less frequently observed is pleural effusion, pneumothorax, or lung lobe consolidation. In seldom occasions, an enlargement of the right ventricle can be distinguished, especially when there is right-sided heart failure (Montoya & Carretón, 2012; American Heartworm Society, 2020; Ware & Ward, 2020). Nevertheless, the morphological changes in some cases are minor or not appreciated in the thoracic radiographies. Moreover, these findings can disappear within months, leaving no infection evidence through radiological study (Stannard, 2015).

According to various scientific articles, computed tomography (CT) is gaining increasing importance as a diagnostic tool for multiple thorax diseases. In the feline species, it has already been used for the description of lung lesions and patterns caused by several respiratory pathologies, such as feline asthma (Masseau *et al*., 2015), feline Aelurostrongylosis (Dennler *et al*., 2013; Lacava *et al*., 2017), mycobacteriosis (Major *et al*., 2015), and even for the description of primary lung neoplasms (Aarsvold *et al*., 2015; Nunley *et al*., 2015).

Despite its high economic cost, CT has higher sensitivity to detect lesions than radiography, since the structures are overlapped in the latter, hampering its visualisation (Prather *et al*., 2005). One of the assets of this diagnostic test is the possibility of creating 3D or multiplane reconstructions in order to have a spatial display and better assessment of the desired anatomical structures. It has also been observed that several factors affect in how the structures will be seen using a contrast medium (contrast enhancement), whether from the patient itself, the injection duration or the velocity of the injection, among others (Drees *et al*., 2014).

Unlike thoracic radiographies, it has been proven that CT is a very useful technique for the identification of bronchiectasis and pulmonary hypertension created by precapillary causes, which are very frequent in cardiopulmonary dirofilariosis (Cannon *et al*., 2013).

In human medicine, CT has a great diagnostic value, since it allows to see and assess lung lesions and nodules associated with *D. immitis* (Oshiro *et al*., 2004; Takei *et al*., 2015). Additionally, this technique is considered the gold standard for the diagnosis of pulmonary thromboembolism in humans (Nikolaou *et al*., 2010). As the CT utility has been demonstrated, it has been used more frequently in veterinary medicine to complement the diagnosis of cardiopulmonary dirofilariosis through the standardisation of measurements and assessment of cardiopulmonary and vascular findings.

The presence of the parasite in the pulmonary vasculature generates proliferative endarteritis (Montoya-Alonso & Carretón-Gómez, 2012). Also, the sudden death of the parasite produces pulmonary thromboembolisms, worsening the vascular damage. Therefore, the pulmonary vascular and bronchial structures are an important subject of study to consider in this pathology. Thus, through previous studies, it has been noted that the relation obtained from the diameter of both the pulmonary trunk and the aorta can be useful to estimate pulmonary hypertension from moderate to severe in dogs parasitised with *D. immitis* (Matos-Rivero *et al*., 2022a). Furthermore, it has also been evaluated the pulmonary vein to pulmonary artery ratio (PV/PA) with CT in canine cardiopulmonary dirofilariosis (Matos-Rivero *et al*., 2022b), since

it allows to detect pulmonary arterial dilation caused by the nematode. As for the bronchus to pulmonary artery ratio (BA), it is also described in clinically healthy dogs (Cannon *et al*., 2009). Research have been conducted using the BA ratio in dogs infected with *D. immitis* to evaluate the pulmonary hypertension (Matos-Rivero *et al*., 2021).

However, in the feline species, there are rather few studies done without animal experimentation to analyse pulmonary lesions and findings associated with *D. immitis* through CT scan. It is only relatively recently when it was described the relation between the bronchus and pulmonary artery in cats with normal lungs, demonstrating its utility to differentiate abnormal bronchi in diseased cats (Reid *et al*., 2012). Likewise, it has been studied bronchial lumen to vertebral body and pulmonary artery to vertebral body ratios in healthy cats (Lee-Fowler *et al*., 2017). Both previous studies were useful to subsequently analyse the same relations in *D. immitis*-infected cats, by using tomographic images (Lee-Fowler *et al*., 2018).

Contrarily, it has not been previously evaluated the bronchial lumen to pulmonary vein (BV), bronchial lumen to pulmonary artery (BA), nor pulmonary vein to pulmonary artery (PV/PA) ratios in naturally infected cats with *D. immitis*. The knowledge extracted from these relations could be useful to know the changes associated with the disease.

1. OBJECTIVES

Evaluate the relations obtained from the BA, BV and PV/PA ratios in a group of feline patients naturally infected with *D. immitis* through CT scan study, in order to analyse the lesions caused by the worm.

MATERIAL AND METHODS

1. Animals

In this study, 24 cats were included, 10 of which were male (41.7%) and 14 female (58.3%). Blood samples from each animal were recollected, including identification data (age, sex and breed) and clinical history. The studied patients ranged from 1 to 15 years old, with an average of 4.32 years. Additionally, all animals showed a similar body weight, being 3.42 kg the average weight. Also, thoracic radiological studies with two projections (right lateral and ventrodorsal) were performed, and it was analysed both hematologic and renal parameters of all patients before going through the general anaesthesia, in order to check the adequate health status.

The study was carried out at the Veterinary Clinical Hospital of the University of Las Palmas de Gran Canaria (ULPGC), and the laboratory of the Department of General Pathology of the ULPGC Veterinary Faculty, between May 2022 and May 2023.

Also, a series of inclusion and exclusion criteria were applied to the feline patients of the study (**Table 3**).

Table 3. Inclusion and exclusion criteria for the feline patients

INCLUSION CRITERIA	EXCLUSION CRITERIA
Animals above 6 months of age	Animals under 6 months of age
Does not take prevention against *D. immitis*	Takes prevention against *D. immitis*
Not on medication when taking the blood sample nor when performing the CT scan	Under medication when taking the blood sample and/or when performing the CT scan

2. Sample collection and assays

The blood samples of the patients, drawn from the cephalic, femoral or jugular vein, were recollected in 2 ml syringes and 21G needles. Afterwards, it was introduced in serum tubes and centrifuged. The serum was kept at -20ºC until its subsequent study.

To detect IgG antibodies against *D. immitis* present in the serum samples of each cat, an indirect ELISA technique was performed (in-house ELISA, UranoVet SL, Barcelona, Spain), following the instructions of the manufacturer.

Figure 2. ELISA protocol execution

Firstly, the serum samples were diluted in the sample diluent buffer (1:100 dilution). Then, 100 µl of each sample was added in the wells of the ELISA plate, which are coated with *D. immitis* recombinant antigens (**Figure 2**). This way, if the sample had specific antibodies against the parasite, these would bind to the antigens in the plate. After 20 minutes, a first well wash was performed to remove the components that did not bind specifically to the antigens.

Afterwards, it was added in each well 100 µL of conjugate, which is an enzyme-linked (peroxidase [HRP]) antibody that binds specifically to the sample antibodies. A second wash step was performed after a 10-minute incubation and, thereupon, the substrate (TMB) was added, a chromogen that produces a blue colour when oxidised, in this case by the action of the peroxidase enzyme. Thus, the wells with antibodies against *D. immitis* will turn blue, being the colour intensity in proportion to the amount of antibodies in the sample.

Finally, 100 µl of stop solution (sulphuric acid) was added in each well to make the reading easier, turning the blue colour to yellow (**Figure 3**). The absorbances (or optical density) were read in a spectrophotometer at 450 nm.

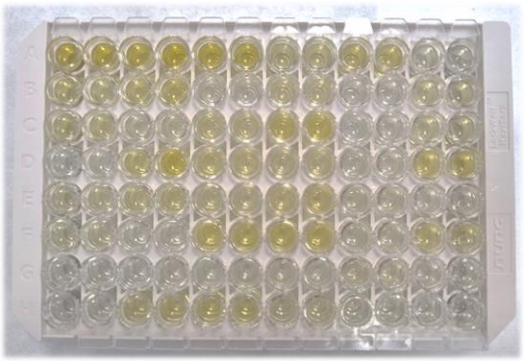

Figure 3. Plate after adding the stop solution

According to the instructions of the manufacturer, the samples with a Cut-Off ≥1 were considered positive to the presence of antibodies against *D. immitis*, whereas those analysed patients with a diagnostic value <1 were negative.

3. CT scan image analysis

Figure 4. Feline patient in sternal recumbency for the CT scan exam

Images were obtained using a helical CT scan (Canon Toshiba Astelion, Canon Medical Systems, Tokyo, Japan). Cats were positioned with their head cranially, in sternal recumbency for image acquisition (**Figure 4**). The anaesthetic protocol was the same for all animals, which included midazolam IV 0.2 mg/kg (Midazolam, B. Braun Medical, Barcelona, Spain) and butorphanol IV 0.2 mg/kg (Torphadine®, Dechra, Northwich, England) as premedication agents, and induction with propofol IV 0.6 mg/kg (Propofol Lipuro®, B. Braun VetCare, Barcelona, Spain). Cats were intubated and anaesthesia was maintained with sevoflurane 2.5% (SevoFlo®, Zoetis, Louvain-la-Neuve, Belgium). Patients were automatically ventilated (General Electric, 9100c NXT – SCIL, Boston, USA) during all the procedure, and vital signs were monitored.

A non-iodinated contrast agent was injected intravenously at a dose of 600 mgI/kg (Xenetix®, Guerbet, Roissy, France) before the acquisition of images. The lung window (window level [WL] –500; window width [WW] 1400) was used for the visualisation and measurement of the lumen of all bronchi, pulmonary arteries and veins. CT images were obtained and reconstructed with a thickness of 1 mm (pitch factor 0.94) and with a soft tissue and bone/lung algorithm. The original data obtained from a transverse plane were used to generate a sagittal and dorsal multiplanar reconstruction (MPR). Measurements were made in the transverse plane at the following locations, according to previously stablished protocols (Reid *et al*., 2012; Lee-Fowler *et al*., 2018): left cranial

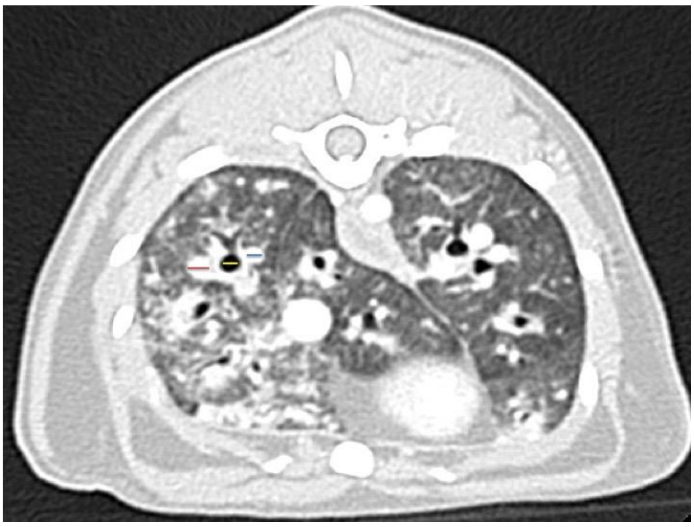

Figure 5. CT image in lung-algorithm (transverse plane) of the thorax of an infected cat at the level between T9 and T10. The lines designate the measurements of the pulmonary artery, bronchial lumen and pulmonary vein (from lateral to medial, respectively) of the right caudal lobe. The left of the patient is to the right of the image.

(cranial segment) and right cranial lobes at T4–T5; middle and left cranial (caudal segment) lobes at T6–T7; and accessory, left caudal and right caudal lobes at T9–T10 (**Figure 5**) intervertebral spaces. The structures were measured transversely. The evaluation of the images was made using the analysis software OsiriX MD. All measurements were carried out by a single researcher.

4. Ethical statement

Owners were informed and gave their consent to participate in this study. The study was carried out according to the actual European legislation for the animal protection.

5. Statistical analysis

For the categorical variables, frequencies and percentages were analysed. Differences in parameters between groups were evaluated with the nonparametric test Pearson's chi-square and, only for the 2x2 tables, the Fisher exact test was applied.

For the continuous variables, the differences in parameters between groups were evaluated with Mann-Whitney/Kruskall-Wallis/Friedman/Wilcoxon tests, due to the low sample size.

All multiple comparisons were adjusted by the Bonferroni correction. All contrasts were accompanied by the effect size estimate to complete the interpretation of the results. The classification of the magnitude of the effect was the following:

- For the continuous variables, Cohen's d: small (d = 0.2 – 0.4), medium (d = 0.5 – 0.8) and large (d > 0.8)
- For the categorical variables, Cramér's V: negligible (0.00 – 0.09), weak (0.10 – 0.29), moderate (0.30 – 0.49) and strong (> 0.50)

Different significance levels were used in the analyses (1% (α=0.01), 5% (α=0.05), 10% (α=0.1)).

Data was analysed using SPSS Base 25.0 Software for Windows.

RESULTS

1. Descriptive study

Based on the serologic results of the animals studied, 18 (75%) were seropositive (Group A), therefore diagnosed with HARD; whereas 6 (25%) were seronegative (Group B), and so were used as healthy animals to have knowledge of the normal physiology.

Significant differences were not observed for the sex, breed, weight and age of any group. Contrarily, there were differences on the clinical signs, so the negatives were asymptomatic and all the positive had respiratory symptoms (**Table 4**).

Table 4. Data of the 24 cats enrolled in the study including clinically healthy cats and cats with cardiopulmonary dirofilariosis.

		RESULT OF THE ELISA TECHNIQUE			
		Total (N%)	**Negative (N%)**	**Positive (N%)**	**p-value**
SEX	**Total**	24 (100.0%)	6 (100.0%)	18 (100.0%)	0.633[1]
	Female	14 (58.3%)	3 (50.0%)	11 (61.1%)	
	Male	10 (41.7%)	3 (50.0%)	7 (38.9%)	
BREED	**Total**	24 (100.0%)	6 (100.0%)	18 (100.0%)	0.185[1]
	European Shorthair	20 (83.3%)	4 (66.7%)	16 (88.9%)	
	Persian	1 (4.2%)	1 (16.7%)	0 (0.0%)	
	Sphynx	3 (12.5%)	1 (16.7%)	2 (11.1%)	
SYMPTOMS	**Total**	24 (100.0%)	6 (100.0%)	18 (100.0%)	0.000[1]; 1.000[2]
	No symptoms	6 (25.0%)	6 (100.0%)	0 (0.0%)	
	Respiratory symptoms	18 (75.0%)	0 (0.0%)	18 (100.0%)	
BODY WEIGHT (kg)	**Valid N**	24	6	18	0.280[3]
	Median	3.42	3.18	3.76	
	Percentile 25	2.84	2.50	3.00	
	Percentile 75	4.55	3.30	4.80	
AGE	**Valid N**	24	6	18	0.673[3]
	Median	4.32	3.78	4.35	
	Percentile 25	2.34	1.02	2.56	
	Percentile 75	8.99	8.36	9.62	

[1] Pearson's Chi square p-value; [2] Cramer's V p-value; [3] Mann-Whitney p-value

2. Comparison of the ratios

A total of 168 sets of ratios (BA, BV and PV/PA) were obtained for all the lung lobes of the studied cats.

To differentiate between lobes, significant differences in the BA and BV ratios existed for the cranial segment of the left cranial lung lobe, for both the negative and positive cats by the ELISA technique (Mann-Whitney U=96, p 0.003 and U=86 p 0.033, respectively). This way, the median values were higher in the positive cats: BA_{median} negatives (RI) = 0.77 [0.68,0.80]

and BA_{median} positives (RI) = 1.00 [0.84,1.33]; BV_{median} negatives (RI) = 0.99 [0.83,1.07] and BV_{median} positives (RI) =1.21 [1.01,1.85] (**Figure 6**); both effects had a large size (d>0.8).

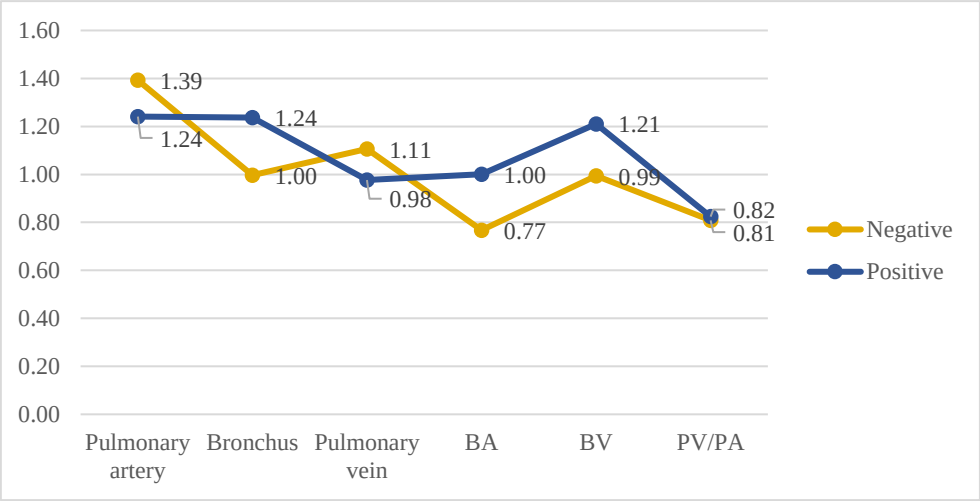

Figure 6. Line chart with median values of the pulmonary artery, bronchus, pulmonary vein and ratios of the cranial segment of the left cranial lung lobe.

In the right cranial lung lobe, significant differences between the BA and BV distributions for the seronegatives and seropositives were observed (Mann-Whitney U=88, p 0.022 and U=82 p 0.066, respectively), so the median values were greater in the positives: BA_{median} negatives (RI) = 0.73 [0.65,0.78] and BA_{median} positives (RI) = 1.13 [0.80,1.55]; BV_{median} negatives (RI) = 0.98 [0.88,1.09] and BV_{median} positives (RI) = 1.36 [0.94,1.62] (**Figure 7**); both effects with a large size (d>0.8).

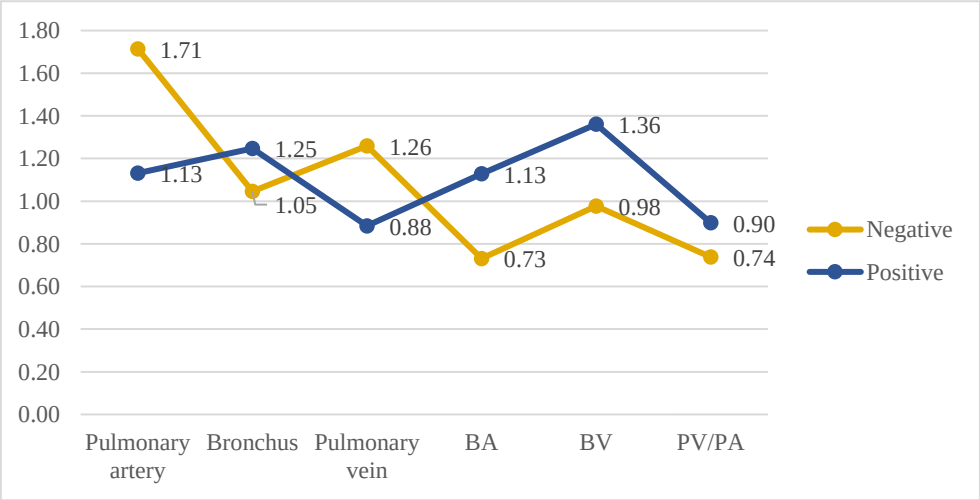

Figure 7. Line chart with median values of the pulmonary artery, bronchus, pulmonary vein and ratios of the right cranial lung lobe.

For the caudal segment of the left cranial lung lobe, significant differences were appreciated for the obtained BA and BV ratios in the negative and positive cats by the ELISA technique (Mann-Whitney U=88, p 0.022 and U=82 p 0.066, respectively). Therefore, the median values

were greater in the positives: BA_{median} negatives (RI) = 0.75 [0.68,0.81] and BA_{median} positives (RI) = 0.99 [0.79,1.48]; BV_{median} negatives (RI) = 1.01 [0.89,1.15] and BV_{median} positives (RI) = 1.25 [1.03,1.66] (**Figure 8**). For BA, the effect size was large, whereas for BV it was medium size.

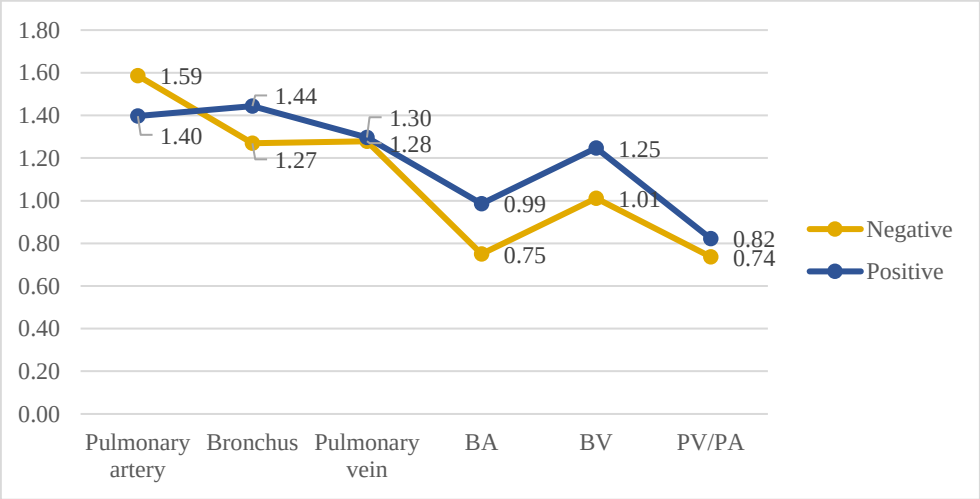

Figure 8. Line chart with median values of the pulmonary artery, bronchus, pulmonary vein and ratios of the caudal segment of the left cranial lung lobe.

The right middle lung lobe showed significant differences between the BA and BV relations for the negative and positive cats by the ELISA technique (Mann-Whitney U=98, p 0.002 and U=88 p 0.022, respectively), so the median values were greater in the positives: BA_{median} negatives (RI) = 0.71 [0.63,0.77] and BA_{median} positives (RI) = 1.00 [0.89,1.24]; BV_{median} negatives (RI) = 0.94 [0.88,1.10] and BV_{median} positives (RI) = 1.14 [1.06,1.66] (**Figure 9**). For BA, both effects had a large size (d>1).

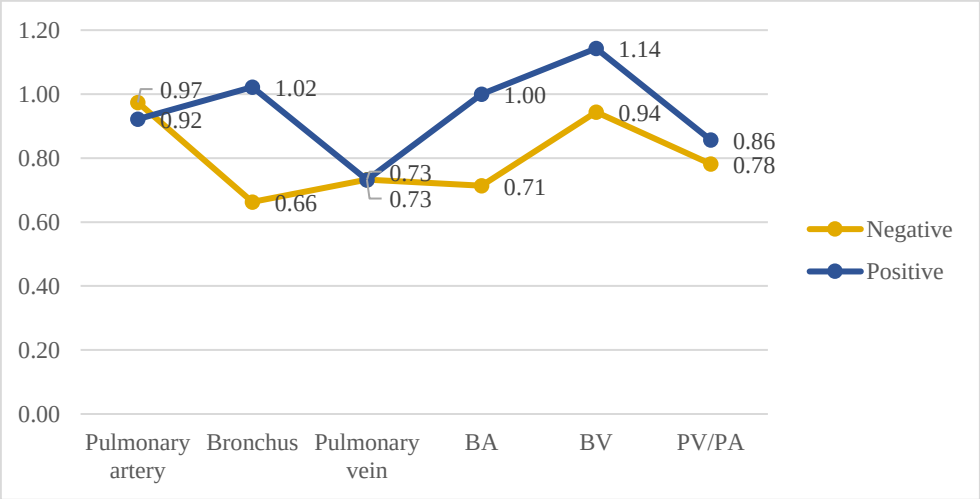

Figure 9. Line chart with median values of the pulmonary artery, bronchus, pulmonary vein and ratios of the right middle lung lobe.

In the case of the left caudal lung lobe, significant differences only existed for the BA relations for the seronegative and seropositive cats (Mann-Whitney U=82, p 0.066), where the median values were greater in the positives: BA_{median} negatives (RI) = 0.72 [0.70,0.83] and BA_{median} positives (RI) = 0.97 [0.80,1.33] (**Figure 10**); both with large effect size (d>1).

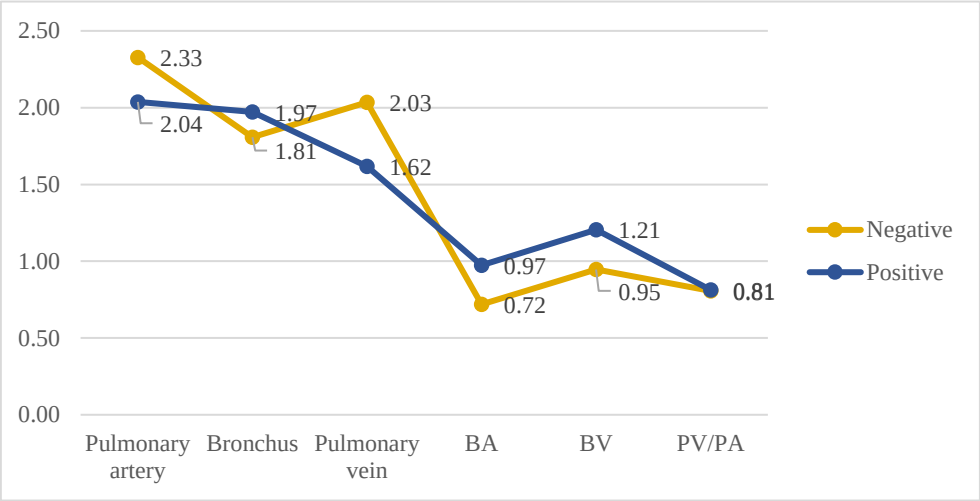

Figure 10. Line chart with median values of the pulmonary artery, bronchus, pulmonary vein and ratios of the left caudal lung lobe.

For the right caudal lung lobe, there were significant differences between the distributions of BA for the negative and positive cats by the ELISA technique (Mann-Whitney U=87, p 0.027). Median values were greater in the positives: BA_{median} negatives (RI) = 0.74 [0.62,0.80] and BA_{median} positives (RI) = 1.06 [0.71,1.38], showing a large effect size. Differences also existed between groups for PA (U=24, p 0.047) and PV (U=24, p 0.047), where values were smaller in the positive cats (**Figure 11**).

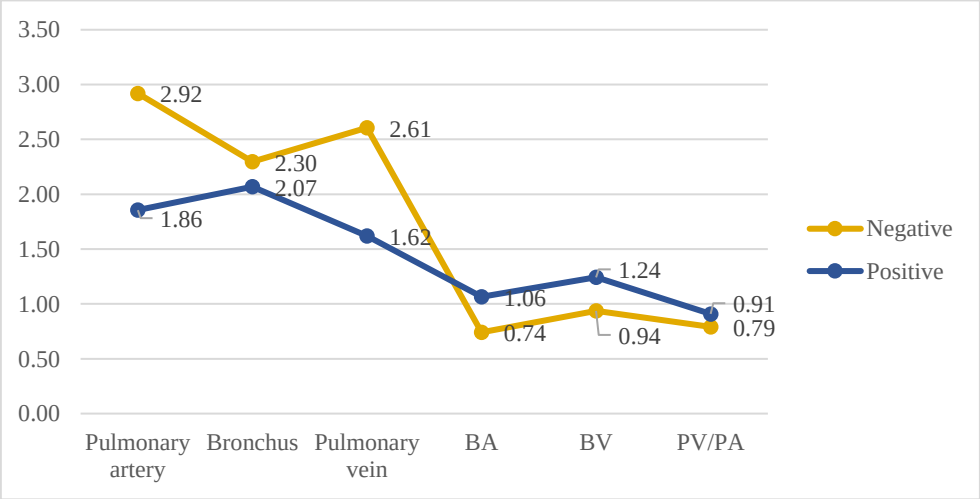

Figure 11. Line chart with median values of the pulmonary artery, bronchus, pulmonary vein and ratios of the right caudal lung lobe.

Lastly, no significant differences existed between groups for any studied parameter in the accessory lung lobe (**Figure 12**).

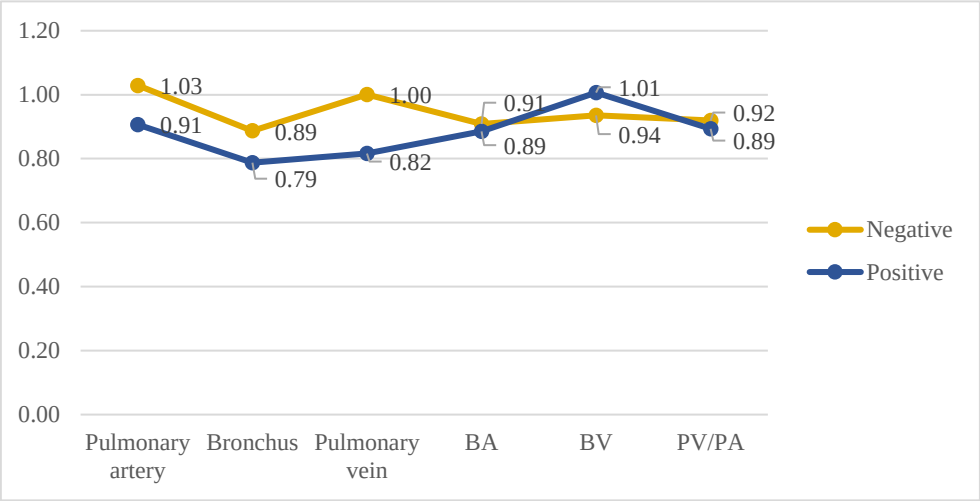

Figure 12. Line chart with median values of the pulmonary artery, bronchus, pulmonary vein and ratios of the accessory lung lobe.

DISCUSSION

The *D. immits* immature larvae trigger an intense lung eosinophilic reaction, which may lead to clinical symptomatology (cough, dyspnoea and tachypnoea, primarily) and radiological signs. Even though cats act as atypical hosts in the *D. immitis* biological cycle, it has been proven a seroprevalence of 9.4% in Spain (Montoya *et al*., 2022a). Its diagnosis is rather complicated due to its similarity with other pathologies of the lower respiratory tract (feline asthma, chronic bronchitis, among others). Thus, the detection of feline cardiopulmonary dirofilariosis has proved to be a tough challenge for many veterinary clinicians, being even underdiagnosed in many places (Rothrock, 2013).

Currently, one the most used serological techniques worldwide for its diagnosis (presumptive and/or definitive) is the ELISA technique, since it allows to detect specific antibodies against the parasite. Additionally, this test has been mainly used for incidence and seroprevalence studies (Montoya-Alonso *et al*., 2011, 2014, 2016, 2017; Villanueva-Saz *et al*., 2021). Other diagnostic tests (antibodies commercial test [Heska®], Knott test, PCR) have also been widely used for the knowledge of prevalences or isolated cases of parasitised cats with *D. immitis* (Venco *et al*., 2008; Park *et al*., 2014; Pană *et al*., 2020; Schäfer *et al*., 2021). However, the rapid test for the detection of antibodies against *D. immitis* (Heska® Solo Step FH; FeliCheck-3, VetExpert) is not commercially available in all countries. Also, PCR and the Knott

test are used for the diagnosis of microfilaraemia, so its usefulness for feline cardiopulmonary dirofilariosis is limited.

Computed tomography is extensively available in veterinary medicine, with a key role in the diagnosis of thoracic diseases in small animals, mainly for the absence of overlapping of thoracic structures and a greater contrast resolution (Armbrust *et al*., 2012). Multiple studies have already demonstrated its ability to evidence feline thorax pathologies (Henninger, 2003; Dennler *et al*., 2013; Aarsvold *et al*., 2015; Major *et al*., 2015; Lacava *et al*., 2017; Panopoulos *et al*., 2019). For cats infected by *D. immitis*, it has been seen that tomographic images show restrictive lung disease, with an increase in the interstitial density and decrease of the total lung volume, where both the bronchi and the pulmonary arteries are damaged (Dillon *et al*., 2014).

In this study, the distribution of the relations obtained by the BA, BV and PV/PA ratios in all lung lobes for the seronegative and seropositive animals were compared. For Group B, significant differences did not exist between lobes in any ratio studied. However, there was between the different lung lobes for the different ratios in the Group A animals.

Regarding the ratio obtained through the bronchial lumen and the pulmonary artery (BA), it has been determined a normal range in dogs of 0.8 – 2.0. With this, bronchi can be considered abnormal in those canine patients that show a BA value > 2.0 (Cannon *et al*., 2009). It has been demonstrated that adult nematodes in the canine species damage the vascular lumen and the elasticity of the pulmonary arteries, blocking the blood flow, and, thus, generating precapillary pulmonary hypertension. Therefore, those dogs that present moderate-severe pulmonary hypertension due to *D. immitis* are exposed to BA relations < 0.8 (Matos-Rivero *et al*., 2021). In humans, a BA relation > 1 has been accepted as superior limit to differentiate normal from dilated bronchi (Hansell, 1998; McGuinness & Naidich, 2002; Reid *et al*., 2012). Likewise, it has also been described the BA ratio in healthy cats, with a mean of 0.71 ± 0.1. A relation ≥0.91 is considered as abnormal bronchi in the feline species (Reid *et al*., 2012). BA ratio in patients with feline asthma has also been studied, where significant differences were not observed as compared to healthy cats (0.93 ± 0.21 and 0.86 ± 0.12, respectively) (Won *et al*., 2017). Nevertheless, a low sample size was presented in the aforementioned study (16 healthy cats and 4 clinically asthmatic cats), as well as variation between breeds, which would justify this absence of significant relation between groups.

Based on the results obtained in this study, significant differences were seen between Group A and Group B cats for the BA ratio in all lung lobes, except for the accessory lobe.

When comparing lung lobes, only seropositive cats showed differences, being the smallest value presented in the accessory lung lobe.

In previous studies, the BA ratio has been assessed in experimentally infected cats, where the bronchial diameter was greater in the right middle and caudal segment of the left cranial lung lobes (Lee-Fowler *et al*., 2018). By contrast, in this study the dilation of the bronchial lumen was mainly seen in the caudal lung lobes. As defined in prior studies, those lung lobes are usually the most affected, since it is where the inflammatory reaction is mainly generated (Montoya-Alonso & Carretón-Gómez, 2012).

Additionally, this preliminary study noticed only significant differences of the BA ratio in the right cranial and left caudal lung lobes (Lee-Fowler *et al*., 2018). In accordance with their results, they concluded that the BA ratio is less reliable when sick cats present changes in both the pulmonary artery and the bronchus, thus generating variations in this ratio.

Notwithstanding, the BA relation in the present study was greater in all lung lobes of all sick cats analysed, as against to the last described values (Lee-Fowler *et al*., 2018). This may be due to the fact that the lumen of the arterial vasculature is not that compromised in cats exposed to the parasite, as compared to the healthy cats. On the other hand, the bronchial lumen of Group A cats was increased in size, which influences the ratio incrementing the value. Moreover, all values, barring the accessory lobe (0.89), were over 0.91, the suggested upper cut-off limit to distinguish between cats apparently healthy from those with bronchial disease (Reid *et al*., 2012). Thereupon, these results reinforce the bronchial reaction that may be generated by the parasite involvement.

Furthermore, diverse investigations have assessed the normal bronchial and pulmonary vascular structures in different terrestrial mammals (Ishaq, 1980; Caccamo *et al*., 2007; Cooley *et al*., 2013; Monteiro & Smith, 2014). Knowing the morphology and physiology of the airways is crucial to distinguish the lung diseases. As regards to cats, it has been observed that pulmonary veins are frequently superior in diameter to the bronchial structure (Panopoulos *et al*., 2019). However, the BV relation has not been described formerly in the feline species. Its use may be of usefulness in cats with venous pulmonary congestion because of cardiac pathologies, poisonings or acute inflammations, as well as to detect bronchial lumen dilation due to a lower respiratory tract pathology that damages its architecture. In the present study, significant differences existed between seropositive and seronegative cats in the cranial and caudal segment of the cranial left, right cranial and right middle lobes. Between lung lobes,

only animals in Group A presented differences, where the lower values belonged to the accessory lung lobe. Therefore, for the aforementioned lobes, these results could be useful as reference values.

Meanwhile, the PV/PA ratio has been greatly utilised in radiological and echocardiographic studies for the diagnosis of venous congestion or pulmonary hypertension (Day & Schull, 2008; Merveille *et al*., 2015; Roels *et al*., 2019). Concretely in the feline species, it has had greater relevance for the diagnosis of left-sided congestive heart failure in hypertrophic cardiomyopathy by echocardiographic study (PV/PA > 0.5) (Patata *et al*., 2020). Additionally, it has shown major repercussion in the canine species for the diagnosis of venous pulmonary congestion caused by myxomatous mitral valve disease (cut-off limit PV/PA 1.7; PV/PA of healthy animals 1.0) (Merveille *et al*., 2015; Birettoni *et al*., 2016) and for the diagnosis of pulmonary hypertension by various aetiologies (Roels *et al*., 2019, 2021). Likewise, this relation has also been used in the canine species in CT study for the diagnosis of pulmonary hypertension caused by pulmonary fibrosis in West Highland White Terriers (Soliveres *et al*., 2021), and, on the other hand, precapillary pulmonary hypertension due to *D. immitis* (0.68 ± 0.18) (Matos-Rivero *et al*., 2022). In the meantime, previous investigations have estimated the diameter of pulmonary veins and arteries using CT in cats free of respiratory symptoms, without implementing the relation PV/PA for the feline species (Panopoulos *et al*., 2019). In these studies, it has been noticed that the pulmonary venous structures own a smaller architecture as compared to the adjacent pulmonary arterial vasculature, as opposed to the canine species (Panopoulos *et al*., 2019).

In the present study, the PV/PA ratio was analysed, where no significant differences were found for any lung lobe for Groups A and B, nor when comparing lung lobes. These results can derive as the pulmonary arteries from the seropositive cats were not so affected compared to the seronegative cats, so alterations in the PV/PA ratio were not observed. A larger feline population could be of great utility to understand if this species could also develop pulmonary hypertension, as it does in the canine cardiopulmonary dirofilariosis.

This study is the first one to describe the relations BA, BV and PV/PA in cats naturally infected with dirofilariosis, in all lung lobes. Nonetheless, it presents limitations regarding certain aspects. The low sample number stands out among them, since the greater the population studied, the more solid the conclusions. Moreover, it is not possible to have knowledge of the exposure time to the parasite nor worm burden in the seropositive cats, with the possibility that

some studied patients were not as affected as others, thus their vascular and bronchial measurements not as altered. Furthermore, a positive antibody result against *D. immitis* can indicate both an active or passive infection. That is, the animal could have HARD, HWD or have recently gone through an infection. In this study, it was not possible to exactly determine what was the case of each animal, being another main limitation. Regarding anaesthesia, the respiratory cycle where images are obtained is key, since ratios obtained using bronchial measurements at the end of expiration are smaller to those obtained in inspiration (Makara *et al*., 2013). Likewise, pulmonary vessels can also be influenced by the respiratory cycle where images are acquired (Lee *et al*., 2022).

In spite of this, these results are of interest to continue investigating bronchial and pulmonary vasculature alterations in cats naturally infected with *D. immitis*. Additionally, due to its difficulty in diagnosis, it is necessary to consider different measures and tests to suspect or presumptively diagnose this pathology in endemic areas. These results also give special importance to the bronchial affection generated by the parasite, being a differential factor in relation to the pathology in the canine species.

CONCLUSIONS

This is the first study to describe values for the BA, BV and PV/PA ratios for all lung lobes in cats naturally infected with *D. immitis*. Based on the results obtained, bronchi were the most affected structures. Thusly, BA and BV ratios can be useful when the bronchial lumen shows alterations in respiratory pathologies, such as HWD or HARD. These results could be of benefit to be included in a diagnostic plan in endemic areas, in order to achieve an appropriate management. Nevertheless, due to the limitations of the study, the results require a cautious approach. More studies should be carried out with a higher sample size to support these results.

Part of the results of this study were presented in: **XXII AVEPA-GTA Congress (April 21-22, 2023 – Bilbao).**

BIBLIOGRAPHY

Aarsvold, S., Reetz, J. A., Reichle, J. K., Jones, I. D., Lamb, C. R., Evola, M. G., Keyerleber, M. A., & Marolf, A. J. (2015). Computed tomographic findings in 57 cats with primary pulmonary neoplasia. *Veterinary Radiology and Ultrasound*, *56*(3), 272–277. https://doi.org/10.1111/vru.12240

American Heartworm Society. (2020). *Current feline guidelines for the prevention, diagnosis, and management of heartworm infection in cats*. American Heartworm Society. www.heartwormsociety.org.

Armbrust, L., Biller, D., Bamford, A., Chun, R., Garrett, L., & Sanderson, M. (2012). Comparison of three-view thoracic radiography and computed tomography for detection of pulmonary nodules in dogs with neoplasia. *Journal of the American Veterinary Medical Association*, *240*(9). https://doi.org/https://doi.org/10.2460/javma.240.9.1088

Birettoni, F., Caivano, D., Patata, V., Moïse, N. S., Guglielmini, C., Rishniw, M., & Porciello, F. (2016). Canine pulmonary vein-to-pulmonary artery ratio: echocardiographic technique and reference intervals. *Journal of Veterinary Cardiology*, *18*(4), 326–335. https://doi.org/10.1016/j.jvc.2016.07.004

Blagburn, B. (2019). *It's so HARD! Feline heartworm case management and diagnostic updates*. VIN. https://www.vin.com/doc/?id=9839094

Caccamo, R., Twedt, D. C., Buracco, P., & McKiernan, B. C. (2007). Endoscopic bronchial anatomy in the cat. *Journal of Feline Medicine and Surgery*, *9*(2), 140–149. https://doi.org/10.1016/j.jfms.2006.10.003

Cannon, M., Johnson, L., Pesavento, P., Kass, P., & Wisner, E. (2013). Quantitative and qualitative computed tomographic characteristics of bronchiectasis in 12 dogs. *Veterinary Radiology and Ultrasound*, *54*(4), 351–357. https://doi.org/10.1111/vru.12036

Cannon, M., Wisner, E., Johnson, L., & Kass, P. (2009). Computed tomography bronchial lumen to pulmonary artery diameter ratio in dogs without clinical pulmonary disease. *Veterinary Radiology and Ultrasound*, *50*(6), 622–624. https://doi.org/10.1111/j.1740-8261.2009.01592.x

Cooley, S. D., Schlipf Jr, J. W., & Stieger-Vanegas, S. M. (2013). Computed tomographic characterization of the pulmonary system in clinically normal alpacas. *American Journal of Veterinary Research*, *74*(4), 572–578. https://doi.org/10.2460/ajvr.74.4.572

Day, J., & Schull, D. (2008). Findings from thoracic radiographs of dogs and cats with tick toxicity. *Australian Veterinarian Practitioner*, *38*(3), 86–91.

DeFrancesco, T., Atkins, C., Miller, M., Meurs, K., & Keene, B. (2001). Use of echocardiography for the diagnosis of heartworm disease in cats: 43 cases (1985-1997). *Journal of the American Veterinary Medical Association*, *218*(1). https://doi.org/https://doi.org/10.2460/javma.2001.218.66

Dennler, M., Bass, D. A., Gutierrez-Crespo, B., Schnyder, M., Guscetti, F., Di Cesare, A., Deplazes, P., Kircher, P. R., & Glaus, T. M. (2013). Thoracic computed tomography, angiographic computed tomography, and pathology findings in six cats experimentally

infected with *Aelurostrongylus abstrusus*. *Veterinary Radiology and Ultrasound*, *54*(5), 459–469. https://doi.org/10.1111/vru.12044

Dillon, A. R., Warner, A. E., Brawner, W., Hudson, J., & Tillson, M. (2008). Activity of pulmonary intravascular macrophages in cats and dogs with and without adult *Dirofilaria immitis*. *Veterinary Parasitology*, *158*(3), 171–176. https://doi.org/10.1016/j.vetpar.2008.09.004

Drees, R., François, C., & Saunders, J. (2014). Invited review-computed tomographic angiography (CTA) of the thoracic cardiovascular system in companion animals. *Veterinary Radiology and Ultrasound*, *55*(3), 229–240. https://doi.org/10.1111/vru.12149

European Society of Dirofilariosis and Angiostrongylosis (ESDA). (2017). *Guidelines for clinical management of feline heartworm disease*. European Society of Dirofilariosis and Angiostrongylosis, 1–5. https://www.esda.vet/index.php/guidelines

Ettinger, S., Feldman, E., & Etienne, C. (2017). Canine and feline heartworm disease. In *Textbook of Veterinary Internal Medicine* (8th ed., pp. 3166–3236). Elsevier.

Hansell, D. M. (1998). Bronchiectasis. *Radiologic Clinics of North America*, *36*(1), 107–128. https://doi.org/10.1016/S0033-8389(05)70009-9

Henninger, W. (2003). Use of computed tomography in the diseased feline thorax. *Journal of Small Animal Practice*, *44*(2), 56–64. https://doi.org/https://doi.org/10.1111/j.1748-5827.2003.tb00121.x

Ishaq, M. (1980). A morphological study of the lungs and bronchial tree of the dog: with a suggested system of nomenclature for bronchi. *Journal of Anatomy*, *131*(Pt 4), 589–610.

Lacava, G., Zini, E., Marchesotti, F., Domenech, O., Romano, F., Manzocchi, S., Venco, L., & Auriemma, E. (2017). Computed tomography, radiology and echocardiography in cats naturally infected with *Aelurostrongylus abstrusus*. *Journal of Feline Medicine and Surgery*, *19*(4), 446–453. https://doi.org/10.1177/1098612X16636419

Lee, J., Chung, J., Baek, L., Je, M., Choi, J., & Yoon, J. (2022). Respiratory phase can affect pulmonary vein-to-pulmonary artery ratio measured with CT. *American Journal of Veterinary Research*, *83*(10). https://doi.org/10.2460/ajvr.22.02.0026

Lee-Fowler, T., Cole, R. C., Dillon, A. R., Graham, S., Tillson, D. M., & Barney, S. (2018). High-resolution CT evaluation of bronchial lumen to vertebral body, pulmonary artery to vertebral body and bronchial lumen to pulmonary artery ratios in *Dirofilaria immitis*-infected cats with and without selamectin administration. *Journal of Feline Medicine and Surgery*, *20*(10), 928–933. https://doi.org/10.1177/1098612X17734999

Lee-Fowler, T., Cole, R., Dillon, A., Tillson, M., Garbarino, R., & Barney, S. (2017). High-resolution computed tomography evaluation of the bronchial lumen to vertebral body diameter and pulmonary artery to vertebral body diameter ratios in anesthetized ventilated normal cats. *Journal of Feline Medicine and Surgery*, *19*(10), 1007–1012. https://doi.org/10.1177/1098612X16668931

Major, A., Holmes, A., Warren-Smith, C., Lalor, S., Littler, R., Schwarz, T., & Gunn-Moore, D. (2015). Computed tomographic findings in cats with mycobacterial infection. *Journal*

of Feline Medicine and Surgery, *18*(6), 510–517. https://doi.org/10.1177/1098612X15588799

Makara, M., Dennler, M., Schnyder, M., Bektas, R., Kircher, P., Hall, E., & Glaus, T. (2013). Effect of ventilation technique and airway diameter on bronchial lumen to pulmonary artery diameter ratios in clinically normal beagle dogs. *Veterinary Radiology and Ultrasound*, *54*(6), 605–609. https://doi.org/10.1111/vru.12073

Masseau, I., Banuelos, A., Dodam, J., Cohn, L. A., & Reinero, C. (2015). Comparison of lung attenuation and heterogeneity between cats with experimentally induced allergic asthma, naturally occurring asthma and normal cats. *Veterinary Radiology and Ultrasound*, *56*(6), 595–601. https://doi.org/10.1111/vru.12267

Matos-Rivero, J. I., Falcón-Cordón, Y., García-Rodríguez, S. N., Costa-Rodríguez, N., Carretón-Gómez, E., & Montoya-Alonso, J. A. (2021, 12-13 November). Evaluación de la hipertensión pulmonar en perros con dirofilariosis cardiopulmonar mediante el uso del ratio broncoarterial. *XVI Andalusian Congress of Veterinarians, Almería, Spain, pp. 85-88*.

Matos-Rivero, J. I., Falcón-Cordón, Y., García-Rodríguez, S. N., Costa-Rodríguez, N., Carretón-Gómez, E., & Montoya-Alonso, J. A. (2022b, 21-26 August). Usefulness of computed tomography PV:PA ratio in the assessment of pulmonary hypertension in dogs with heartworm disease. XV *International Congress of Parasitology (ICOPA), Copenhagen, Denmark, pp. 549*.

Matos-Rivero, J. I., Falcón-Cordón, Y., García-Rodríguez, S. N., Costa-Rodríguez, N., Montoya-Alonso, J. A., & Carretón, E. (2022a). Evaluation of pulmonary hypertension in dogs with heartworm disease using the computed tomographic pulmonary trunk to aorta diameter ratio. *Animals*, *12*(18), 2441. https://doi.org/10.3390/ani12182441

McGuinness, G., & Naidich, D. P. (2002). CT of airways disease and bronchiectasis. *Radiologic Clinics of North America*, *40*(1), 1–19. https://doi.org/10.1016/S0033-8389(03)00105-2

Merveille, A.-C., Bolen, G., Krafft, E., Roels, E., Gomart, S., Etienne, A.-L., Clercx, C., & Mc Entee, K. (2015). Pulmonary Vein-to-Pulmonary Artery Ratio is an Echocardiographic Index of Congestive Heart Failure in Dogs with Degenerative Mitral Valve Disease. *Journal of Veterinary Internal Medicine*, *29*(6), 1502–1509. https://doi.org/10.1111/jvim.13634

Monteiro, A., & Smith, R. L. (2014). Bronchial tree architecture in mammals of diverse body mass. *International Journal of Morphology*, *32*(1), 312–316. https://doi.org/10.4067/S0717-95022014000100050

Montoya-Alonso, J. A., & Carretón-Gómez, E. (2012). *Dirofilariosis: Pautas de Manejo Clínico*. Multimédica Ediciones Veterinarias.

Montoya-Alonso, J. A., Carretón, E., Corbera, J. A., Juste, M. C., Mellado, I., Morchón, R., & Simón, F. (2011). Current prevalence of *Dirofilaria immitis* in dogs, cats and humans from the island of Gran Canaria, Spain. *Veterinary Parasitology*, *176*(4), 291–294. https://doi.org/10.1016/j.vetpar.2011.01.011

Montoya-Alonso, J. A., Carretón, E., García-Guasch, L., Expósito, J., Armario, B., Morchón, R., & Simón, F. (2014). First epidemiological report of feline heartworm infection in the

Barcelona metropolitan area (Spain). *Parasites and Vectors*, *7*, 506. https://doi.org/10.1186/s13071-014-0506-6

Montoya-Alonso, J. A., Carretón, E., Morchón, R., Silveira-Viera, L., Falcón, Y., & Simón, F. (2016). The impact of the climate on the epidemiology of *Dirofilaria immitis* in the pet population of the Canary Islands. *Veterinary Parasitology*, *216*, 66–71. https://doi.org/10.1016/j.vetpar.2015.12.005

Montoya-Alonso, J. A., García-Rodríguez, S. N., Carretón, E., Rodríguez-Escolar, I., Costa-Rodríguez, N., Matos, J. I., & Morchón, R. (2022a). Seroprevalence of feline heartworm in spain: completing the epidemiological puzzle of a neglected disease in the cat. *Frontiers in Veterinary Science*, *9*. https://doi.org/10.3389/fvets.2022.900371

Montoya-Alonso, J. A., Morchón, R., Falcón-Cordón, Y., Falcón-Cordón, S., Simón, F., & Carretón, E. (2017). Prevalence of heartworm in dogs and cats of Madrid, Spain. *Parasites and Vectors*, *10*(1), 354. https://doi.org/10.1186/s13071-017-2299-x

Montoya-Alonso, J. A., Morchón, R., García-Rodríguez, S. N., Falcón-Cordón, Y., Costa-Rodríguez, N., Matos, J. I., Rodríguez-Escolar, I., & Carretón, E. (2022b). Expansion of canine heartworm in spain. *Animals*, *12*(10), 1268. https://doi.org/10.3390/ani12101268

Morchón, R., Ferreira, A. C., Martín-Pacho, J. R., Montoya, A., Mortarino, M., Genchi, C., & Simón, F. (2004). Specific IgG antibody response against antigens of *Dirofilaria immitis* and its *Wolbachia* endosymbiont bacterium in cats with natural and experimental infections. *Veterinary Parasitology*, *125*(3–4), 313–321. https://doi.org/10.1016/j.vetpar.2004.08.003

Nikolaou, K., Thieme, S., Sommer, W., Johnson, T., & Reiser, M. F. (2010). Diagnosing pulmonary embolism new computed tomography applications. *Journal of Thoracic Imaging*, *25*(2), 151–160. https://doi.org/10.1097/RTI.0b013e3181d9ca1d

Nunley, J., Sutton, J., Culp, W., Wilson, D., Coleman, K., Demianiuk, R., Schechter, A., Moore, G., Donovan, T., & Schwartz, P. (2015). Primary pulmonary neoplasia in cats: Assessment of computed tomography findings and survival. *Journal of Small Animal Practice*, *56*(11), 651–656. https://doi.org/10.1111/jsap.12401

Oshiro, Y., Murayama, S., Sunagawa, U., Nakamoto, A., Owan, I., Kuba, M., Uehara, T., Miyahira, T., Kawabata, T., Kuniyoshi, M., Ishikawa, K., Kinjyo, T., Fujimoto, K., & Yamada, K. (2004). Pulmonary dirofilariasis computed tomography findings and correlation with pathologic features. *Journal of Computed Assisted Tomography*, *28*(6), 796–800. https://doi.org/10.1097/00004728-200411000-00011

Pană, D., Rădulescu, A., Mitrea, I. L., & Ionita, M. (2020). First report on clinical feline heartworm (*Dirofilaria immitis*) infection in Romania. *Helminthologia*, *57*(1), 49–56. https://doi.org/10.2478/helm-2020-0009

Panopoulos, I., Auriemma, E., Specchi, S., Diana, A., Pietra, M., Papastefanou, A., Zini, E., & Cipone, M. (2019). 64-multidetector CT anatomical assessment of the feline bronchial and pulmonary vascular structures. *Journal of Feline Medicine and Surgery*, *21*(10), 893–901. https://doi.org/10.1177/1098612X18807778

Park, H.-J., Lee, S.-E., Lee, W.-J., Oh, J.-H., Maheswaran, E., Seo, K.-W., & Song, K.-H. (2014). Prevalence of *Dirofilaria immitis* infection in stray cats by nested PCR in Korea. *The Korean Journal of Parasitology*, *52*(6), 691–694. https://doi.org/10.3347/kjp.2014.52.6.691

Patata, V., Caivano, D., Porciello, F., Rishniw, M., Domenech, O., Marchesotti, F., … Birettoni, F. (2020). Pulmonary vein to pulmonary artery ratio in healthy and cardiomyopathic cats. *Journal of Veterinary Cardiology*, *27*, 23–33. https://doi.org/10.1016/j.jvc.2019.12.001

Prather, A., Berry, C., & Thrall, D. (2005). Use of radiography in combination with computed tomography for the assessment of noncardiac thoracic disease in the dog and cat. *Veterinary Radiology and Ultrasound*, *46*(2), 114–121. https://doi.org/10.1111/j.1740-8261.2005.00023.x

Ray Dillon, A., Tillson, D. M., Wooldridge, A., Cattley, R., Hathcock, J., Brawner, W. R., … Schachner, E. R. (2014). Effect of pre-cardiac and adult stages of *Dirofilaria immitis* in pulmonary disease of cats: CBC, bronchial lavage cytology, serology, radiographs, CT images, bronchial reactivity, and histopathology. *Veterinary Parasitology*, *206*(1–2), 24–37. https://doi.org/10.1016/j.vetpar.2014.09.007

Reid, L., Ray Dillon, A., Hathcock, J., Brown, L., Tillson, M., & Wooldridge, A. (2012). High-resolution computed tomography bronchial lumen to pulmonary artery diameter ratio in anesthetized ventilated cats with normal lungs. *Veterinary Radiology and Ultrasound*, *53*(1), 34–37. https://doi.org/10.1111/j.1740-8261.2011.01870.x

Roels, E., Fastrès, A., Merveille, A.-C., Bolen, G., Teske, E., Clercx, C., & Mc Entee, K. (2021). The prevalence of pulmonary hypertension assessed using the pulmonary vein-to-right pulmonary artery ratio and its association with survival in West Highland white terriers with canine idiopathic pulmonary fibrosis. *BMC Veterinary Research*, *17*(1), 171. https://doi.org/10.1186/s12917-021-02879-w

Roels, E., Merveille, A.-C., Moyse, E., Gomart, S., Clercx, C., & Mc Entee, K. (2019). Diagnostic value of the pulmonary vein-to-right pulmonary artery ratio in dogs with pulmonary hypertension of precapillary origin. *Journal of Veterinary Cardiology*, *24*, 85–94. https://doi.org/10.1016/j.jvc.2019.06.001

Rothrock, K. (2013, November 7). *Dirofilariasis (Heartworm Disease) (Feline)*. VIN. https://www.vin.com/doc/?id=6041077&pid=607

Schäfer, I., Kohn, B., Volkmann, M., & Müller, E. (2021). Retrospective evaluation of vector-borne pathogens in cats living in Germany (2012–2020). *Parasites & Vectors*, *14*(1), 123. https://doi.org/10.1186/s13071-021-04628-2

Simón, F., Siles-Lucas, M., Morchón, R., González-Miguel, J., Mellado, I., Carretón, E., & Montoya-Alonso, J. A. (2012). Human and animal dirofilariasis: The emergence of a zoonotic mosaic. *Clinical Microbiology Reviews*, *25*(3), 507–544. https://doi.org/10.1128/CMR.00012-12

Soliveres, E., Mc Entee, K., Couvreur, T., Fastrès, A., Roels, E., Merveille, A.-C., … Bolen, G. (2021). Utility of computed tomographic angiography for pulmonary hypertension assessment in a cohort of west highland white terriers with or without canine idiopathic

pulmonary fibrosis. *Frontiers in Veterinary Science*, *8*. https://doi.org/10.3389/fvets.2021.732133

Stannard, R. (2015). The facts about feline heartworm disease. *Today's Veterinary Practice*, *5*(1), 93–98.

Takei, D., Yamaki, M., Noriyuki, T., Takemoto, Y., Kawashima, M., Saitoh, R., Sasada, T., Yoshida, M., Amano, H., Fukuda, T., Nakahara, M., & Masuda, K. (2015). Lung canine filariasis diagnosed by postoperative pathology. *Kyobu Geka. The Japanese Journal of Thoracic Surgery*, *68*(1), 76–79.

Turb, M. E., Zambon, E., Zannoni, A., Russo, S., & Gentilini, F. (2012). Detection of *Wolbachia* DNA in blood for diagnosing filaria-associated syndromes in cats. *Journal of Clinical Microbiology*, *50*(8), 2624–2630. https://doi.org/10.1128/JCM.00528-12

Venco, L., Mortarino, M., Carro, C., Genchi, M., Pampurini, F., & Genchi, C. (2008). Field efficacy and safety of a combination of moxidectin and imidacloprid for the prevention of feline heartworm (*Dirofilaria immitis*) infection. *Veterinary Parasitology*, *154*(1–2), 67–70. https://doi.org/10.1016/j.vetpar.2008.02.020

Villanueva-Saz, S., Giner, J., Verde, M., Yzuel, A., González, A., Lacasta, D., Marteles, D., & Fernández, A. (2021). Prevalence of microfilariae, antigen and antibodies of feline dirofilariosis infection (*Dirofilaria immitis*) in the Zaragoza metropolitan area, Spain. *Veterinary Parasitology: Regional Studies and Reports*, *23*. https://doi.org/10.1016/j.vprsr.2021.100541

Walden, H., & Estrada, A. (2019). *Dirofilaria immitis Diagnosis and Heartworm Associated Respiratory Disease in Cats*. VIN. https://www.vin.com/doc/?id=9052481

Ware, W., & Ward, J. (2020). Hipertensión pulmonar y dirofilariosis. In *Medicina interna de pequeños animales* (6th ed., pp. 193–207). Edra.

Winter, R. L., Ray Dillon, A., Cattley, R. C., Blagburn, B. L., Michael Tillson, D., Johnson, C., … Barney, S. (2017). Effect of heartworm disease and heartworm-associated respiratory disease (HARD) on the right ventricle of cats. *Parasites and Vectors*, *10*. https://doi.org/10.1186/s13071-017-2451-7

Won, S., Yun, S., Lee, J., Lee, M., Choi, M., & Yoon, J. (2017). High resolution computed tomographic evaluation of bronchial wall thickness in healthy and clinically asthmatic cats. *Journal of Veterinary Medical Science*, *79*(3), 567–571. https://doi.org/10.1292/jvms.16-0476